Toxicol Res. (2021) 37:261–275
https://doi.org/10.1007/s43188-020-00063-0

eISSN 2234-2753
pISSN 1976-8257

ORIGINAL ARTICLE

Hepatoprotective effect of *Centella asiatica* 50% ethanol extract against acetaminophen-induced acute liver injury in BALB/c mice

Dae Won Park[1,2] · Hyelin Jeon[2,3] · Jeong Eun Kwon[1,2] · Young Geun Lee[1] · Rina So[1,2] · Tae Hwan Choe[1,2] · Yong Joon Jeong[3] · Se Chan Kang[1,2]

Received: 19 May 2020 / Revised: 12 August 2020 / Accepted: 21 August 2020 / Published online: 7 September 2020

Abstract

N-acetyl-*p*-aminophenol (acetaminophen, APAP) is a well-known component of analgesic and antipyretic monotherapy products. However, exceeding the recommended dose can lead to serious injury to the liver. We conducted this study to determine the potential of *Centella asiatica* as a natural substance to protect against APAP-induced liver injury. When acute hepatotoxicity was induced in mice by APAP overdose, their liver weight decreased significantly ($p < 0.05$). However, mice treated with *C. asiatica* 50% ethanol extract (CA-HE50, 200 mg/kg) for a week before induction of hepatotoxicity by APAP had similar liver weights to those of mice in which hepatotoxicity was not induced. In particular, levels of aspartate aminotransferase, alanine aminotransferase, and lactate dehydrogenase, which are biomarkers of liver injury, were significantly increased by APAP and dose-dependently decreased by CA-HE50 ($p < 0.05$). Glutathione and malondialdehyde, indicators of oxidative stress, were significantly changed by APAP and CA-HE50 ($p < 0.05$). In addition, hepatic necrosis and expression of genes encoding pro-inflammatory cytokines (tumor necrosis factor-α, interleukin (IL)-1β, and IL-4) induced by APAP were inhibited by CA-HE50, and these results were dose-dependent. Through our in vivo studies, we found that CA-HE50 can help prevent APAP-induced hepatic tissue injury in BALB/c mice. Furthermore, CA-HE50 was effective at protecting RAW 264.7 cells from lipopolysaccharide-induced cytotoxicity and inhibiting the release of nitric oxide from these cells; in particular, asiaticoside was found to be a key component of CA-HE50 responsible for these effects. Therefore, we suggest that CA-HE50 has potential applications in functional health foods and drugs.

Keywords *Centella asiatica* · Triterpenoids · Asiaticoside · *N*-acetyl-*p*-aminophenol · Acute liver failure · Hepatoprotective activity

Dae Won Park and Hyelin Jeon contributed equally to this work as co-first authors.

✉ Se Chan Kang
sckang@khu.ac.kr

Dae Won Park
dw@nmr.kr

Hyelin Jeon
iljhl@hanmail.net

Jeong Eun Kwon
jjung@nmr.kr

Young Geun Lee
lyg629@nate.com

Rina So
sorina@nmr.kr

Tae Hwan Choe
615speed@nmr.kr

Yong Joon Jeong
jeyoon@genencell.co.kr

[1] Department of Oriental Medicine Biotechnology, College of Life Sciences, Kyung Hee University, 1732, Deogyeong-daero, Giheung-gu, Yongin, Gyeonggi-do 17104, Republic of Korea

[2] BioMedical Research Institute, Kyung Hee University, Yongin, Gyeonggi-do 17104, Republic of Korea

[3] Genencell Co. Ltd., Yongin, Gyeonggi-do 16950, Republic of Korea

Introduction

Drug-induced liver injury (DILI) is a clinical problem that is a major concern worldwide [1]. Most DILI cases and acute liver failure (ALF) are caused by accidental overdose of the drug *N*-acetyl-*p*-aminophenol (acetaminophen, APAP) [2]. APAP (in the United States), also known as paracetamol (in Europe and other areas of the world), is one of the most commonly used compounds worldwide; since 1955, its use as an antipyretic or analgesic drug has become mainstream, particularly because it is easily accessible in various formulations as a prescription-free medication [3]. Reported cases of APAP-induced hepatotoxicity first emerged in the United States in the mid-1980s. Moreover, APAP has been reported to be one of the most common pharmaceutical products to cause DILI [3–5]. When used at therapeutic doses, APAP is metabolized by glucuronidation or sulfation into stable metabolites, and/or by the cytochrome p450 system into the reactive metabolite *N*-acetyl-*p*-benzoquinone imine (NAPQI). Under normal circumstances, NAPQI is rapidly converted to nontoxic metabolites by a glutathione (GSH) transferase-dependent pathway. However, with large doses of APAP, NAPQI levels increase and NAPQI may react with hepatic proteins, resulting in liver injury [6, 7]. In addition, an APAP overdose causes activation of immune cells and acute inflammation, leading to ALF [2]. In general, APAP induces hepatic failure at doses exceeding 150 mg/kg, but several studies have reported that lower doses can also cause acute liver injury and liver failure [3–5, 8, 9]. APAP-induced hepatic injury can be studied in animal models, and most mechanisms are translatable to humans [2, 10].

Research to prevent or suppress liver injury caused by drugs is ongoing [11], and investigating the potential of natural products as drugs for the treatment of various diseases is attracting the interest of many researchers. Many bioactive substances with pharmacological activities are synthesized from constituents of essential oils (a mixture of volatile and natural substances) [12]. We focused on *Centella asiatica*, a clonal perennial herbaceous creeper belonging to the family *Apiaceae* (*Umbelliferae*), that has a wide range of traditional, medicinal, and therapeutic values. *Centella asiatica* is found in swampy area in most tropical and subtropical countries and is indigenous to warmer regions of both hemispheres including India, Sri Lanka, South East Asia, parts of China, Western South Sea Islands, Mexico, South East USA, South Africa, Columbia, Eastern South America, Venezuela, and Madagascar [13]. *Centella asiatica* is an ethnomedicinally important plant, used all over the world for the treatment of cholera, jaundice, diarrhea, hepatitis, syphilis, measles, toothache, smallpox, asthma, urethritis, renal stones, rheumatism, varicose veins, neuralgia, anorexia, leprosy, and skin diseases due to its analgesic, antipyretic, and anti-inflammatory properties [14]. However, there have been no scientific reports on the effects of *C. asiatica* extract on APAP-induced hepatotoxicity. We therefore investigated the therapeutic effects of *C. asiatica* extract in an animal model of APAP-induced liver injury.

Materials and methods

Preparation of CA-HE50

Centella asiatica was collected from Hapcheon-gun (Gyeongsangnam-do, Korea) in August 2017, and was identified by Professor Kang Se Chan, Kyung Hee University (Yongin, Gyeonggi-do, Korea). A voucher specimen (JBR536) was deposited in the Laboratory of Natural Medicine Resources in the BioMedical Research Institute, Kyung Hee University. The extract was analyzed in the following manner. *Centella asiatica* was washed three times with distilled water and then dried while avoiding direct sunlight and pulverized. Crude extract was obtained by extracting dried *C. asiatica* twice with 15 times and 5 times the weight of *C. asiatica* of 50% ethanol for 8 h and 6 h, at 80 °C, respectively. Extracts were concentrated to 20 ~ 25 Brix at reduced pressure and 65 °C using a rotary evaporator, and then the crude extract was spray-dried to obtain powder and stored at − 20 °C until use. We refer to *C. asiatica* 50% ethanol extract as 'CA-HE50' (Lot #. 20171123) throughout this manuscript. When administered orally to experimental animals, CA-HE50 was mixed with 0.9% normal saline.

In vivo *experiments*

Animal care: Induction of APAP-induced hepatic injury and treatment with CA-HE50

Fifty 5-week-old male BALB/c strain mice were purchased from NARA Biotech Co. Ltd. (Seoul, Korea) and were allowed to acclimatize for 1 week prior to experiments. Animals were maintained under standard laboratory conditions: temperature of 22 ± 3 °C, relative humidity of 50 ± 5%, and a regular photoperiod (12-h dark/light). Experimental procedures and animal care protocols were approved by the Animal Care and Use Committee of Kyung Hee University and complied with the Guide for the Care and Use of Laboratory Animals of the National Institutes of Health (NIH Publication No. 85-23). Animal experiments were performed in accordance with the current ethical regulations for animal care and use at Kyung Hee University (KHUASP-18-009). Experimental animals were divided into five groups of 10

animals each. Group I received 0.9% saline by oral administration (NC, normal control), Group II received 0.9% saline and 200 mg/kg APAP by oral administration (APAP, vehicle control), while Groups III–V received CA-HE50 (50, 100, and 200 mg/kg) and 200 mg/kg APAP by oral administration. APAP 200 mg/kg was given by oral administration on the last day of the experiment (the 7th day), and mice were fasted for 12 h before delivery to maximize the induction of liver toxicity. Animals were sacrificed 24 h after APAP was provided. Mice were euthanized by CO_2 gas, and body weights were measured at the beginning and end of experiments. Organ weights of the sacrificed animals were also measured. Serum samples and liver tissue were collected, and subjected to biochemical and histological analyses.

Measurement of liver function markers

After the completion of experiments, blood was collected from the mice, and serum was obtained by centrifugation. To determine liver health, we measured levels of eight liver biomarkers using commercial ELISA kits according to the manufacturer's instructions. In more detail, levels of aspartate aminotransferase (AST, Sigma-Aldrich, St. Louis, MO, USA), alanine aminotransferase (ALT, Sigma-Aldrich), alkaline phosphatase (ALP, Abcam, Milton, Cambridge, UK), lactate dehydrogenase (LDH, Abcam), albumin (ALB, Abcam), γ-globulin (Abcam), total-bilirubin (T-BIL, Abcam), and total bile acid (TBA, Biovision, Milpitas, CA, USA) in the serum were measured.

Homogenization of liver tissue to assess liver function parameters

Livers were washed, minced, and homogenized in a Dounce glass homogenizer in 10 mM HEPES–KOH/1 mM EGTA buffer (pH 7.5) containing 250 mM sucrose and supplemented with protease and phosphatase inhibitors. Homogenates were spun down for 10 min at 2000 g at 4 °C. Supernatant was collected and used for ex vivo experiments. These homogenates were used to determine glutathione (GSH) and malondialdehyde (MDA) levels using GSH and MDA activity assay kits purchased from Cell Biolabs, Inc. (San Diego, CA, USA) according to the manufacturer's instructions.

Histological staining

At the time of sacrifice, small pieces of liver tissue were harvested and fixed immediately in 10% buffered formalin phosphate and 4% paraformaldehyde (Sigma-Aldrich), and then embedded in paraffin. For histological examination, 5 µm-thick sections were prepared from paraffin blocks using a Reichert 200 microtome (Leica, Nussloch, Eisfeld, Germany) and mounted on glass slides. Sections were then stained with hematoxylin (Sigma-Aldrich) and eosin (Sigma-Aldrich) to evaluate injury and inflammation. Histopathological changes were examined under a light microscope (Nikon, Tokyo, Japan), photographs were taken at 200 × magnification.

Quantitative real-time PCR analysis

Total RNA was extracted and purified from liver tissue with TRIzol reagent (Invitrogen, Waltham, MA, USA). Yield and purity of RNA were determined from the absorbance value at 260 nm (A260) and the A260/A280 ratio. Then, 1 µg of total RNA in a 20 µL volume was transcribed using the PrimeScriptII 1st strand cDNA Synthesis kit (Takara, Tokyo, Japan). Quantitative real-time (qRT)-PCR reactions targeting mouse cytochrome p450 2E1 (CYP2E1), monocyte chemoattractant protein 1 (MCP1), interleukin (IL)-1β, IL-4, IL-6, IL-10, tumor necrosis factor (TNF)-α, and β-actin were performed on an MX3005P thermocycler (Stratagene, La Jolla, CA, USA). Primers used in the experiments are shown in Table 1. For qRT-PCR analysis, SYBR Premix Ex Taq II (Takara) was used. The final reaction volume was 25 µL comprising 2 µL cDNA template, 12.5 µL of SYBR premix, 1 µL each primer (10 µM stock solution), and 9.5 µL sterile distilled water. Thermal cycling profile consisted of a pre-incubation step at 95 ℃ for 10 min followed by 40 cycles of 95 ℃ (15 s), 58 ℃ (1 min), 72 °C (1 min), and then 72 °C for 10 min. Relative expression of the biomarkers was determined using the comparative cycle threshold (CT) method.

Table 1 Sequences of the primers used for qRT-PCR analysis

Gene name	Primer Sequence
CYP2E1	5′-GTTGCCTTGCTTGTCTGGAT-3′ (sense)
	5′-AGGAATTGGGAAAGGTCCTG-3′ (antisense)
MCP1	5′-GTCAAGCCAGACGAAGAACA -3′ (sense)
	5′-TGGACCCATTCCTTCTTGGG -3′ (antisense)
TNF-α	5′-GTCTACTGAACTTCGGGGTGAT-3′ (sense)
	5′-ATGATCTGAGTGTGAGGGTCTG-3′ (antisense)
IL-1β	5′-GCAACTGTTCCTGAACTCAACT-3′ (sense)
	5′-ATCTTTTGGGGTCCGTCAACT-3′ (antisense)
IL-4	5′-ACGGAGATGGATGTGCCAAAC-3′ (sense)
	5′-AGCACCTTGGAAGCCCTACAGA-3′ (antisense)
IL-6	5′-TGGAGTCACAGAAGGAGTGGCTAAG-3′ (sense)
	5′-TCTGACCACAGTGAGGAATGTCCAC-3′ (antisense)
IL-10	5′-ATGGTGTCCTTTCAATTGCTCT-3′ (sense)
	5′-AGGATCTCCCTGGTTTCTCTTC-3′ (antisense)
β-actin	5′-TGTCCACCTTCCAGCAGATGT-3′ (sense)
	5′-AGCTCAGTAACAGTCCGCCTAGA-3′ (antisense)

In vitro *experiments*

Cell culture and cytotoxicity assay

RAW 264.7 murine macrophage cells were obtained from the American Type Culture Collect (ATCC, Manassas, VA, USA). RAW 264.7 cells were cultured in Dulbecco's modified Eagle's medium (DMEM, Gibco, Grand Island, NY, USA) supplemented with inactivated 10% fetal bovine serum (FBS, Hyclone, South Logan, UT, USA) and 1% penicillin/streptomycin (Gibco) in a 37 °C incubator with a 5% CO_2 atmosphere. Cytotoxicity was determined by 3-(4,5-dimethylthiazol-2-yl)-2,5-diphenyltetrazolium bromide (MTT) assay. In brief, cells were seeded at a density of 3.5×10^4 cells/well in 96-well plates. After incubation overnight, cells were treated with CA-HE50 or components of CA-HE50 (asiatic acid, AA; asiaticoside, AS; madecassic acid, MA; and madecassoside, MS) for 22 h. Then, 1 μg/mL lipopolysaccharide (LPS, Sigma-Aldrich) was added to cells for 2 h. Cells were then incubated with 10 μL of 5 mg/mL MTT (Sigma-Aldrich) for 4 h. After the supernatant was removed, 150 μL of dimethyl sulfoxide (DMSO, Sigma-Aldrich) was added per well to dissolve the formazan crystals and the plate was shaken twice for 4 to 5 s. Optical density (OD) was measured at a 570 nm using a multi-reader plate reader (TECAN, Männedorf, Switzerland). Cytotoxicity was expressed as a percentage relative to untreated control cells.

Nitric oxide measurement

RAW 264.7 cells (2×10^5 cells/well) were seeded in 96-well plates and incubated overnight. Then, cells were treated with 20 μg/mL CA-HE50 and four components of CA-HE50 at three different concentrations (5, 10, and 20 μg/mL) for 22 h after which they were stimulated with 1 μg/mL LPS for 2 h. After this, 100 μL of the supernatant was removed from each well and placed into an empty 96-well plate and then 100 μL of Griess reagent (1% sulfanilamide and 0.1% naphthylethylenediamine dihydrochloride in 2.5% phosphoric acid, Sigma-Aldrich) was added to each well. Absorbance was measured at 550 nm using a microplate reader (Bio-Rad Laboratories, Hercules, CA, USA).

Metabolite profiling of CA-HE50 using UHPLC-QTOF/MSMS

UHPLC was performed using the UltiMate™ 3000 Rapid Separation Binary System (Thermo Fisher Scientific Inc., Waltham, MA, USA) with a Phenomenex F5 C18 column (2.6 μm, 2.1 × 100 mm). The column oven was maintained at 40℃, and mobile phases were solvent A [0.1% FA in water (v/v)] and solvent B [0.1% FA in acetonitrile (*v*/*v*)]. Elution gradient was as follows: 0–1 min, B 5%; 1–17 min, B 5–100%; 17–20 min, B 100%; 20–21 min, B 100–5%; 21–25 min, B 5%. Flow rate was 0.25 mL/min, and the injection volume was 5 μL for each run. MSMS analysis was performed using a Triple TOF 5600^+ (AB Sciex Pte. Ltd., Framingham, MA, USA) operating in positive and negative ion mode. Mass spectrometers performed alternating high- and low-energy scans, known as the MS^E acquisition mode. Operating parameters were as follows: MS scan type, full scan and information dependent acquisition (IDA) scanning; ionization source, electrospray ionization (ESI); MS scan range, 50–1500 m/z; MS/MS scan range, 50–1500 m/z; nebulizing gas, 50 psi; heating gas, 50 psi; curtain gas, 25 psi; desolvation temperature, 500 ℃; ion-spray voltage floating, 5.5 kV; declustering potential, 60 V; collision energy, 35 V; cone gas flow 30 L/h; and desolvation gas flow, 800 L/h.

In addition, a UHPLC system with a Phenomenex F5 C18 column was used to profile various metabolites of CA-HE50; these metabolites were well separated within 10–30 min at a flow of 0.25 mL/min. Total ion chromatograms (TIC) of CA-HE50 were analyzed using UHPLC-QTOF/MSMS; data were then processed using Scaffold 4 (Proteome Software Inc., Portland, Oregon, USA) software. Peaks were selected based on ID and a mass accuracy score > 0.80.

HPLC analysis of asiaticoside

CA-HE50 was analyzed by HPLC using an Agilent 1260 Infinity separation module coupled to a DAD detector (Agilent Technologies, Santa Clara, CA, USA), a Cadenza-CD18 C18 (3 μm, 4.6 × 250 mm) column (IMTAKT, Portland, OR, USA), and flow rate of 1.0 mL/min. The column was placed in a column oven at 40 °C. Ratios of mobile phases A (distilled water) and B (acetonitrile) were changed after 0 (90:10, v/v), 10 (80:20, v/v), 40 (73:27, v/v), 45 (80:20, v/v), 51 (20:80, v/v), and 55 (90:10, v/v) min. Injection volume was 10 μL, and UV detection was performed at 206 nm. Different components of CA-HE50 were confirmed by LC–MS. Confirmation of CA-HE50 compound content was performed using the external standard method and asiaticoside (Cat. # CFN99912, ChemFaces, Wuhan, Hubei, China) as the standard stock solution (15.625, 31.25, 62.5, 125, 250, and 500 μg/mL). HPLC-grade acetonitrile, water (Fisher Scientific Korea, Seoul, Korea), and methanol (Duksan, Ansan-si, Gyeonggi-do, Korea) were used.

Statistical analysis

All experimental results are expressed as mean ± standard error of the mean (SEM) of several independent experiments. Statistical significance of group differences was determined by one-way analysis of variance (ANOVA), and individual differences between the means of groups were

analyzed using Student's *t*-test. SPSS Statistics 12.1 K software (IBM) was used for statistical analyses, and *p* values less than 0.05 were considered significant.

Results

CA-HE50 suppresses APAP-induced organ injury

Many ALF patients develop renal complications, cardiopulmonary complications, and/or infections that can progress to multi-organ failure [15]. Therefore, the goal of our research group is to find natural substances (with low toxicity) that can treat or prevent hepatic injury caused by APAP; in this study, we describe our findings for *C. asiatica*. Before proceeding with this study, we conducted a safety evaluation using rodents to determine appropriate conditions to use. By conducting the 'single and 14-day repeated oral study in rodents', we confirmed that the non-toxic amount of CA-HE50 was 2 g/kg/day (data not shown). Therefore, we conducted a study on the protective effect of CA-HE50 on the liver using CA-HE50 doses of 50, 100, and 200 mg/kg/day. The body weight of the experimental animals euthanized with CO_2 and the main organ weights are shown graphically in Fig. 1. First, there was no statistically significant difference in the body weights of the experimental animals at the start and end of the experiment, nor were there significant differences between groups (Fig. 1a). Usually, when liver failure is induced, liver hypertrophy and edema occur due to the burden of metabolism in the liver. Furthermore, the liver, kidneys, and/or spleen can hypertrophy [15]. As shown in Fig. 1b, our study confirmed that the weight of the liver was reduced when APAP was administered to induce liver toxicity ($p < 0.05$). Roberts et al. reported that when APAP induced liver toxicity, a reduction in liver weight occurred between 6 and 24 h, and was associated with an increase in serum ALT and AST levels, indicating liver cell lysis [16]. Similar to this previous study, we provided APAP and weighed the liver 24 h later. Serum levels of ALT and AST were significantly increased, suggesting lysis of hepatocytes (Fig. 2a, b). Therefore, the decrease in liver weight caused by APAP in our study was likely due to liver cell injury (lysis) caused by APAP toxicity. Provision of 200 mg/kg CA-HE50, however, prevented the APAP-induced decrease in liver weight. Thus CA-HE50 helps to protect against liver injury. Kidney and spleen weight were increased by APAP toxicity, which CA-HE50 protected against, but these increases in weight upon APAP treatment were not statistically significant (Fig. 1c, d).

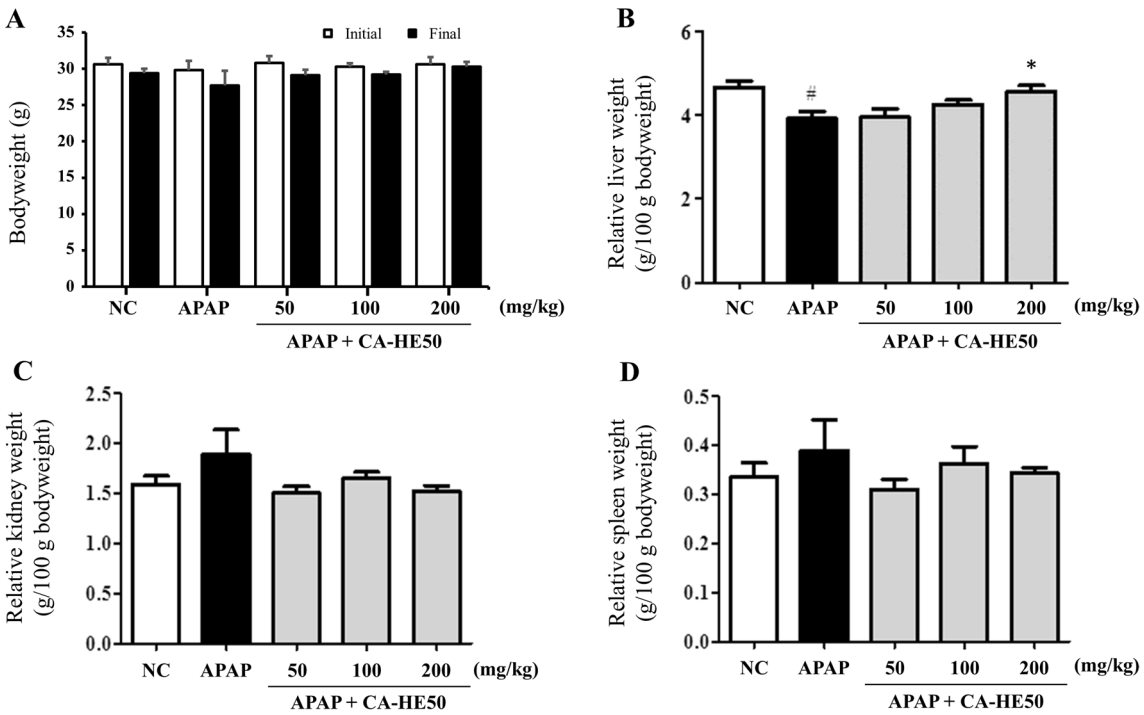

Fig. 1 Body weights and major organ weights of experimental animals. **a** body weight; **b** relative liver weight (g/100 g body weight); **c** relative kidney weight (g/100 g body weight); **d** relative spleen weight (g/100 g body weight). Data are expressed as means ± SEMs ($n = 10$) and were analyzed using one-way ANOVA. #significantly different from NC ($p < 0.05$), *significantly different from APAP ($p < 0.05$). *NC* normal control (0.9% saline); *APAP* vehicle control (0.9% saline + 200 mg/kg APAP p.o.); CA-HE50 50 (50 mg/kg CA-HE50 + APAP); CA-HE50 100 (100 mg/kg CA-HE50 + APAP); CA-HE50 200 (200 mg/kg CA-HE50 + APAP)

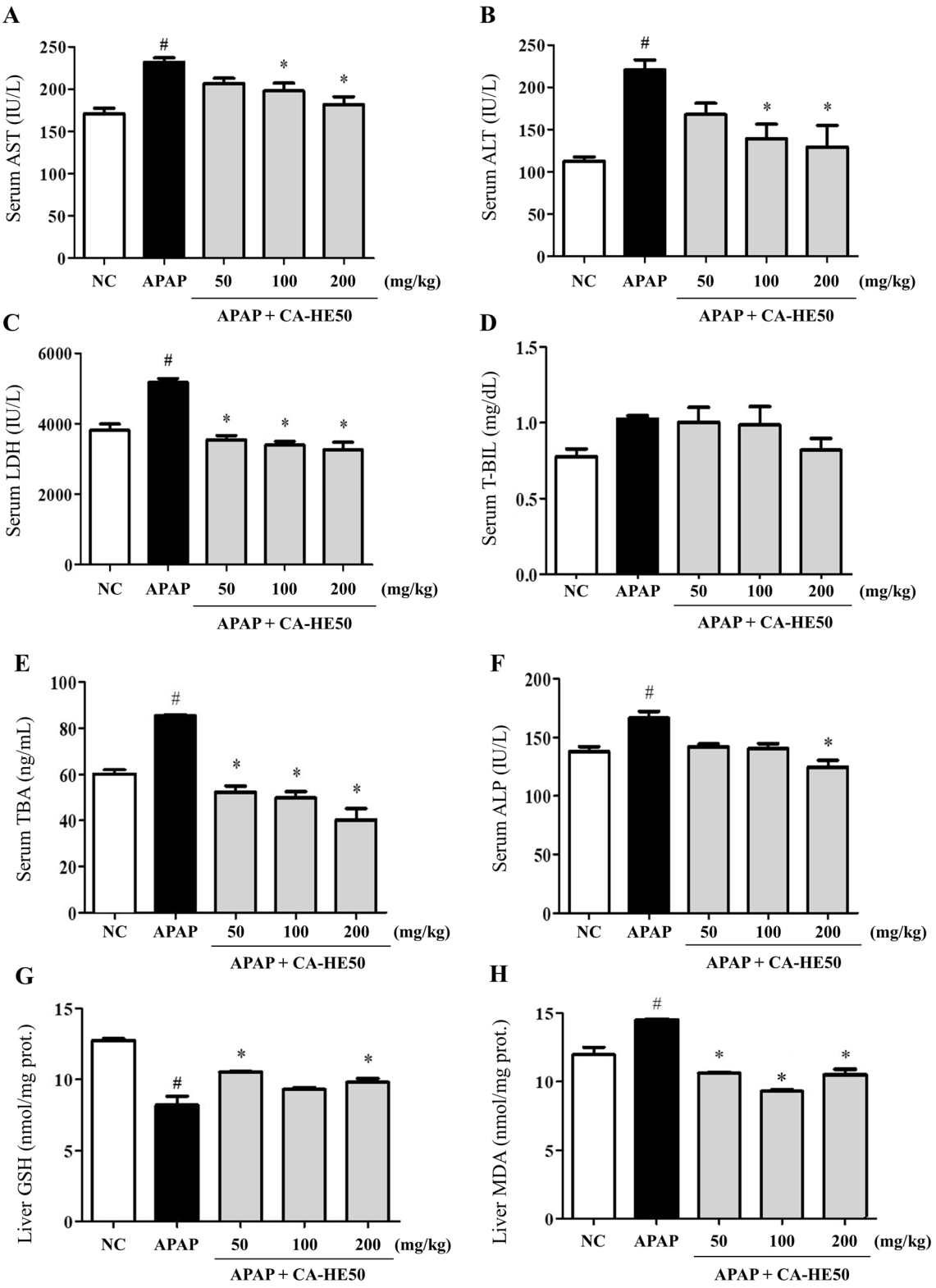

CA-HE50 prevents hepatocyte injury

Detection of one or more biomarkers in the setting of hepatotoxicity is desirable, especially in clinical scenarios where the diagnosis of APAP hepatotoxicity can be complicated. Multiple serum biomarkers of hepatotoxicity have been proposed to identify not only hepatocyte injury and necrosis, but also to help predict patient outcomes [17, 18]. Biochemical

◂**Fig. 2** Effect of CA-HE50 on APAP-induced hepatocyte injury. **a** aspartate aminotransferase (AST) levels in serum; **b** alanine aminotransferase (ALT) levels in serum; **c** lactate dehydrogenase (LDH) levels in serum. **d** total bilirubin (T-BIL) levels in serum; **e** total bile acid (TBA) levels in serum. **f** alkaline phosphatase (ALP) levels in serum; **g** liver glutathione (GSH) storage level; **h** liver malondialdehyde (MDA) accumulated level. Data are expressed as means ± SEMs ($n = 10$) and were analyzed using one-way ANOVA. $^{\#}$significantly different from NC ($p < 0.05$), *significantly different from APAP ($p < 0.05$). *NC* normal control (0.9% saline); *APAP* vehicle control (0.9% saline + 200 mg/kg APAP p.o.); CA-HE50 50 (50 mg/kg CA-HE50 + APAP); CA-HE50 100 (100 mg/kg CA-HE50 + APAP); CA-HE50 200 (200 mg/kg CA-HE50 + APAP)

tests called liver function tests (LFTs) usually include measurement of AST, ALT, ALP, ALB, and T-BIL levels. ALT and AST levels in serum reflect hepatic injury, while level of ALB and prothrombin time and γ-globulin level reflect liver synthesis functions. T-BIL level reflects hepatic excretory function. In this study, we used 10 biomarkers to determine hepatocyte injury. As shown in Fig. 2a and b, AST and ALT levels in the serum were greatly increased after APAP-induced hepatotoxicity. However, in mice that received CA-HE50 prior to APAP treatment, serum ALT and AST levels decreased in a CA-HE50 dose-dependent manner and were significantly different ($p < 0.05$). ALT is more specific for hepatocyte injury than AST. As shown in Fig. 2b, CA-HE50 helped prevent hepatic cell injury by significantly reducing serum ALT levels ($p < 0.05$). LDH is an enzyme that plays an essential role in energy production. It is known to be present in the liver, heart, kidney, and red blood cells [19]. When diseases occur in these organs, the serum LDH level is increased. Serum LDH levels were dramatically increased by APAP overdose but were significantly decreased when CA-HE50 was given first (Fig. 2c). These results suggest that CA-HE50 protects against APAP-induced hepatocyte injury. In addition to hepatocyte injury, levels of ALB and γ-globulin were also checked to determine the overall synthesis functions of the liver. These two indicators change mainly in patients with chronic liver disease [20]. No significant difference in these indicators was observed among groups (data not shown).

CA-HE50 suppresses intrahepatic cholestasis

T-BIL, TBA, and ALP were measured to determine the effects of CA-HE50 on liver detoxification ability and bile acid secretion/uptake. T-BIL levels reflect the detoxifying/secretion abilities of the liver, and serum T-BIL levels increase upon chemical injury to the liver. Severe jaundice symptoms occur when the serum T-BIL level is high [21]. As shown in Fig. 2d, T-BIL levels tended to increase with APAP but decreased after CA-HE50 treatment in a concentration-dependent manner, but these differences were not statistically significant. Serum levels of TBA were significantly increased by APAP overdose, but were dramatically decreased in all groups that received CA-HE50 versus the control ($p < 0.05$) (Fig. 2e), likely because CA-HE50 suppresses the secretion of ALP, which is elevated in bile acid excretion disorders (Fig. 2f). Based on the above results, we concluded that APAP overdose can cause bile acid excretion disorders and that CA-HE50 can protect against this by inhibiting ALP secretion. In particular, TBA levels in the CA-HE50 treatment groups were lower than in the normal control group, suggesting that CA-HE50 can promote bile acid reabsorption.

CA-HE50 inhibits lipid peroxidation in the liver

We measured the levels of the antioxidant GSH and the oxidative stress marker MDA, which are involved in oxidative stress in the liver [21]. NAPQI is initially detoxified by conjugation with GSH to form mercapturic acid [22]. Thus, GSH as a non-enzymatic antioxidant is one of the first lines of defense against APAP toxicity. GSH removes free radical species such as hydrogen peroxide (H_2O_2) and superoxide radicals to maintain the integrity of membrane protein thiols, and is a substrate for glutathione peroxidase (GPx) and glutathione-*s*-transferase (GST) [23]. It also provides a hub for the effective functioning of other antioxidant systems. The CA-HE50-mediated reversal of the APAP-induced decrease in GSH levels strongly indicates that CA-HE50 is a potent antioxidant that protects against oxidative stress and hepatotoxicity. As shown in Fig. 2g, APAP overdose depleted GSH, but pre-treatment with high and low doses of CA-HE50 protected against this ($p < 0.05$). The anti-oxidant effect of CA-HE50 was further confirmed by the significant suppression of MDA levels by CA-HE50. In the present study, the APAP-induced decrease in levels of GSH was associated with an elevation in the end products of lipid peroxidation, such as MDA. As shown in Fig. 2h, a significant increase in the formation of MDA was observed in the livers of mice overdosed with APAP ($p < 0.05$). However, pre-treatment with CA-HE50 suppressed the APAP-induced increase in MDA. We attributed these results to the antioxidant effects of numerous phytochemicals present in CA-HE50.

CA-HE50 inhibits histopathological liver injury

To visually confirm the ability of CA-HE50 to protect against APAP-induced hepatic tissue injury, we performed hematoxylin and eosin (H&E, Sigma-Aldrich) staining of liver tissues. Areas of injured liver tissue area are enlarged and shown to the right of the panels in Fig. 3. The magnified area of each panel is characterized in that the shape of the cell or the boundary of the nucleus is not correctly identified. H&E staining confirmed injury to liver cells due to APAP, but hypertrophy due to edema of the liver and steatosis in

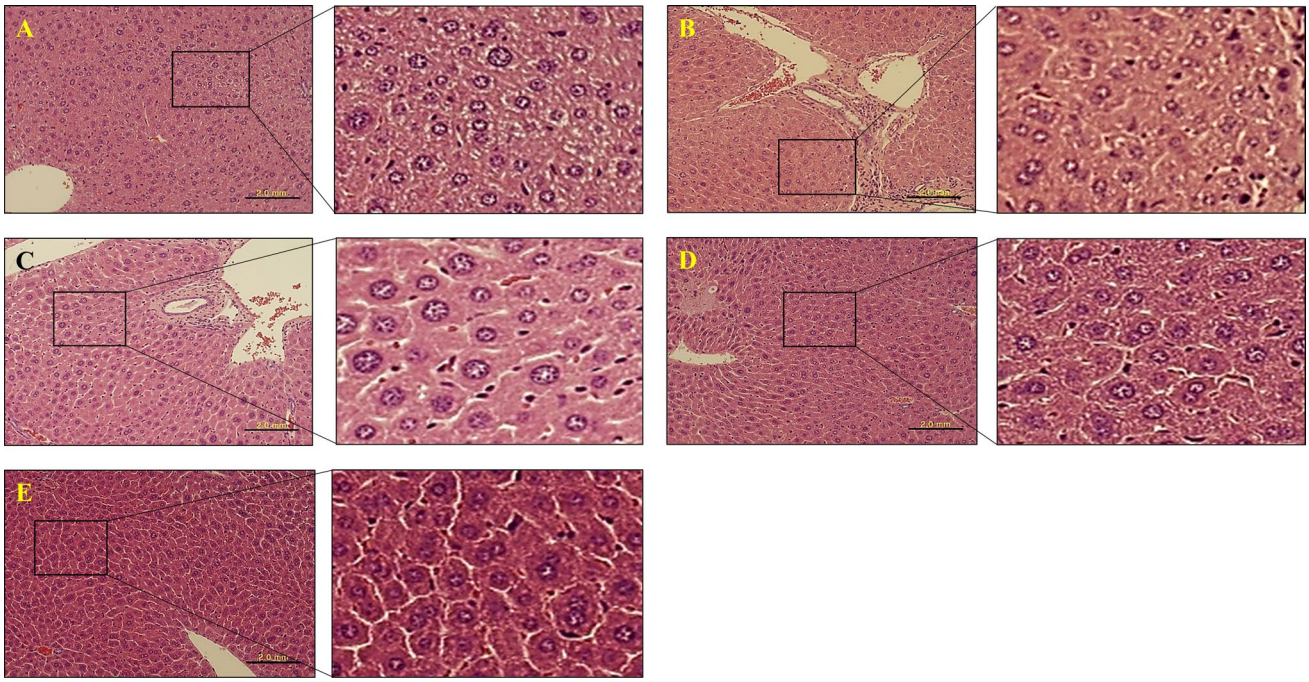

Fig. 3 Histological analysis of liver tissue. Pictures were taken at 200× magnification, and the scale bar represents 2.0 mm (left panel). **a** Normal control (0.9% saline); **b** vehicle control (0.9% saline + 200 mg/kg APAP p.o.); **c** CA-HE50 50 (50 mg/kg CA-HE50 + APAP); **d** CA-HE50 100 (100 mg/kg CA-HE50 + APAP); **e** CA-HE50 200 (200 mg/kg CA-HE50 + APAP)

the liver due to fat accumulation were not observed (see Fig. 3, panel b). These results were judged to be because of APAP-induced acute liver injury (necrosis). By contrast, CA-HE50 protected the livers of treated groups in a dose-dependent manner (panels c–e). In particular, mice treated with 200 mg/kg CA-HE50 group (panel e) had liver cells that were indistinguishable from those of the normal control group (panel a).

CA-HE50 suppresses inflammatory gene expression

Expression levels of CYP2E1, MCP1, TNF-α, IL-1β, IL-4, IL-6, and IL-10 in mice liver tissue were measured and results are shown in Fig. 4. As expected, real time-PCR analysis confirmed that over-administration of APAP promoted CYP2E1, MCP1, IL-1β, IL-4, and TNF-α gene expression. However, expression of these five genes was suppressed in a concentration-dependent manner when CA-HE50 was provided ($p < 0.05$). As shown in Fig. 4a, 50 mg/kg CA-HE50 tended to suppress CYP2E1 expression, while 200 mg/kg CA-HE50 significantly suppressed CYP2E1 expression ($p < 0.01$). Similar to CYP2E1, the gene expression of MCP1 was dramatically suppressed by treatment with 50 mg/kg CA-HE50, and this suppression was statistically significant at 100 and 200 mg/kg CA-HE50 ($p < 0.05$) (Fig. 4b). TNF-α expression was dramatically reduced by treatment with all concentrations of CA-HE50, but this suppression was only statistically significant at 200 mg/kg CA-HE50 (Fig. 4c). Similarly, expression of IL-1β was significantly suppressed by all doses of CA-HE50, and IL-1β expression was lower in all groups that received CA-HE50 than the normal control group (Fig. 4d). A CA-HE50 dose of 200 mg/kg significantly suppressed IL-4 expression (Fig. 4e). However, as shown in Fig. 4f and g, CA-HE50 did not appear to affect the expression of IL-6 and IL-10.

Pharmacologically active components of CA-HE50

Analytical tests were conducted to determine the components present in CA-HE50. We identified 88 phytochemicals present in CA-HE50 by UHPLC-QTOF/MSMS analysis (Fig. 5). Among the 88 types of phytochemicals, saccharides such as sucrose, D-fructose, and stachyose, and amino acids including D-glutamate, adenosine, and *β*-leucine were observed. Flavonoids such as quercetin, kaempferol, and scutellarin were also detected. Additionally, we confirmed the presence of triterpenoid saponins (AA, AS, MA, and MS), which are well known functional components of *C. asiatica* (Table 2).

Cell protective efficacy of triterpenoid saponins

Among the 88 components identified, those components expected to have a protective effect against liver toxicity

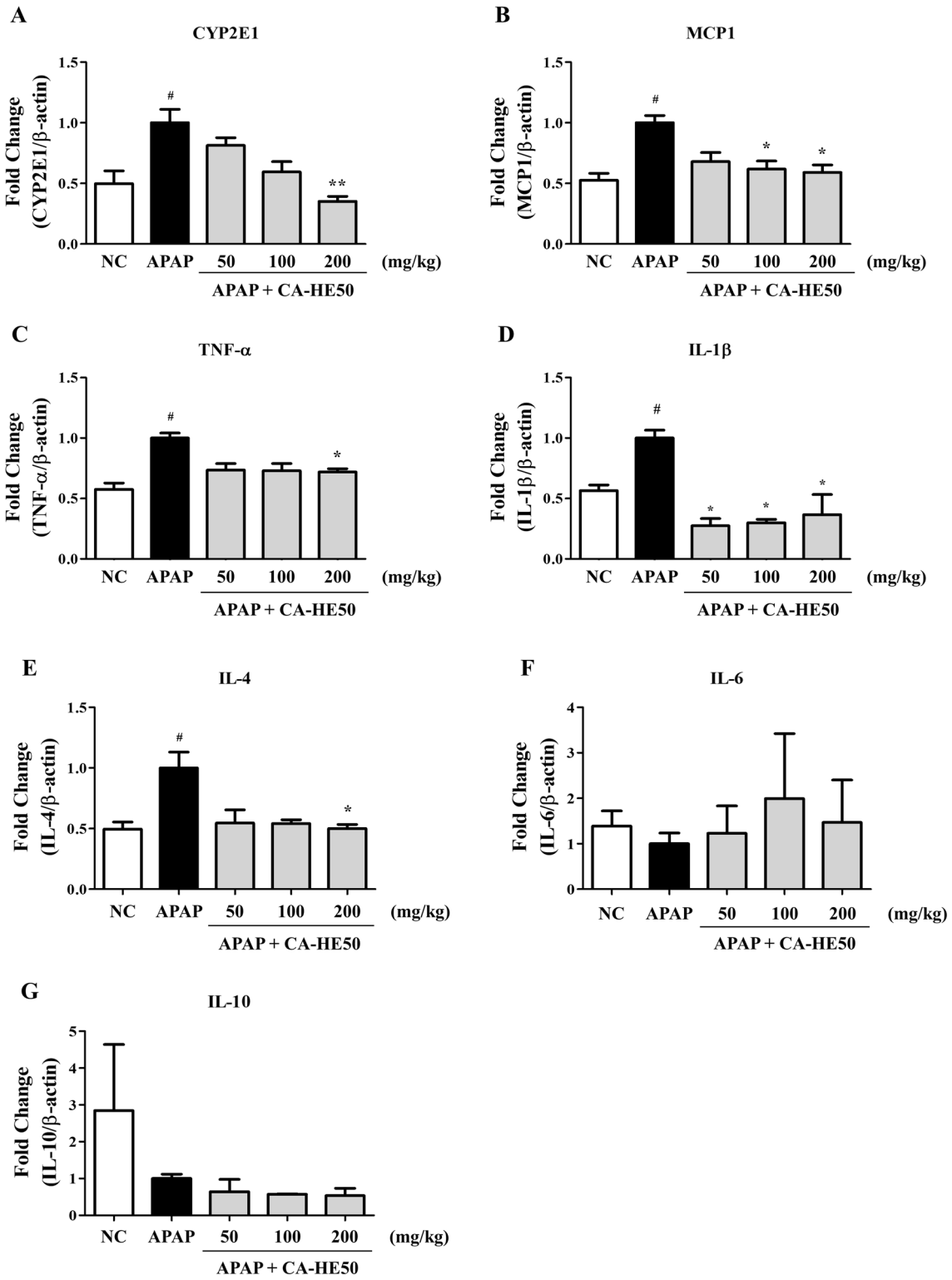

Fig. 4 Inhibitory effects of CA-HE50 administration on pro-inflammatory cytokine and chemokine expression. **a** CYP2E1; **b** MCP1; **c** TNF-α; **d** IL-1β; **e** IL-4; **f** IL-6; **g** IL-10. Data are expressed as means ± SEMs ($n = 10$) and were analyzed using one-way ANOVA. #significantly different from NC ($p < 0.05$), *significantly different from vehicle control ($p < 0.05$), **significantly different from vehicle control ($p < 0.01$). *NC* normal control (0.9% saline); *APAP* vehicle control (0.9% saline + 200 mg/kg APAP p.o.); CA-HE50 50 (50 mg/kg CA-HE50 + APAP); CA-HE50 100 (100 mg/kg CA-HE50 + APAP); CA-HE50 200 (200 mg/kg CA-HE50 + APAP)

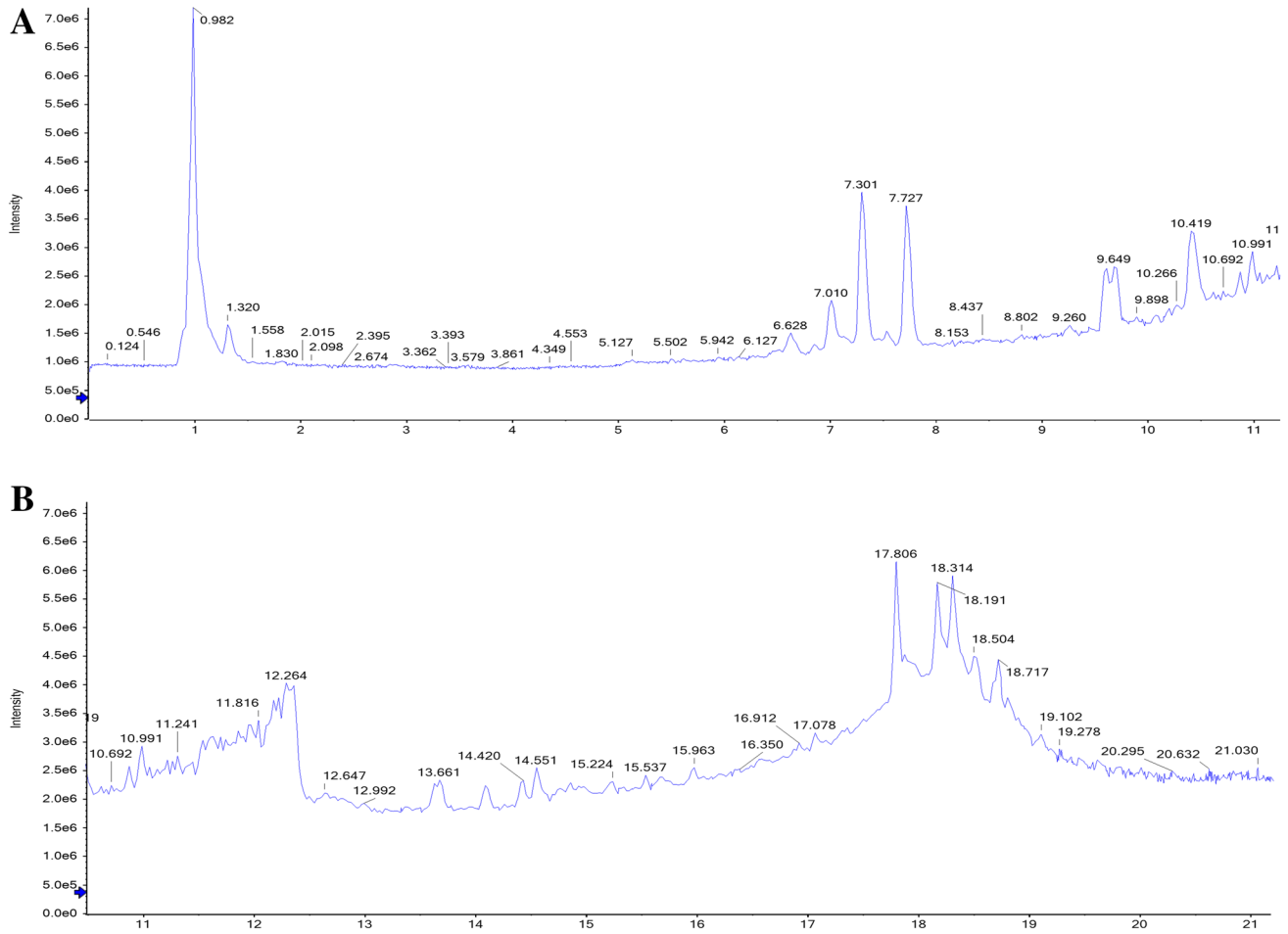

Fig. 5 UHPLC-QTOF/MSMS chromatogram of *Centella asiatica* 50% ethanol extract (CA-HE50). Eight-eight phytochemicals were identified

were selected (triterpenoid saponins), and in vitro experiments performed. As shown in Fig. 6a, all four of these components significantly increased the viability of RAW 264.7 cells stimulated with LPS ($p < 0.05$). Among these, AS had a significant protective effect on cell viability at a concentration of 20 µg/mL. In the NO release inhibition experiments, 10 µg/mL ($p < 0.05$) and 20 µg/mL ($p < 0.01$) AA acid and AS had more marked inhibitory effects than MA or MS (Fig. 6b). Previous studies have demonstrated that AS has antioxidant and anti-inflammatory properties [24, 25] in addition to wound healing and anti-apoptosis activity [26]. AS is a triterpenoid saponin series that is a well characterized active ingredient of *C. asiatica* [27, 28]. Based on our results, we attribute the ability of CA-HE50 to protect liver cells to AS.

Components of CA-HE50

We confirmed the content of AS in CA-HE50 by HPLC (Fig. 7). A peak of AS was verified at 41.6 min, and the AS content of CA-HE50 was found to be 14.4 ± 0.25 mg/g.

Discussion

APAP is one of the most widely used antipyretic analgesic drugs worldwide, but excess amounts of this compound can lead to acute liver injury [4]. In the United States, 82,000 emergency room visits and 26,000 hospitalizations occur yearly due to APAP overdose [29]. Furthermore, liver toxicity caused by APAP is the leading cause of acute liver injury and ALF in the United States, accounting for 50% of all ALF cases [30]. The United States Food and Drug Administration (FDA) recommends providing N-acetylcysteine (NAC) to protect against APAP overdose toxicity. However, complex infusion therapy is required for treatment of APAP overdose, and is associated with a high incidence of side-effects, including anaphylactic reactions [31]. Therefore, new preventative or therapeutic drugs for liver injury caused by APAP are needed. As part of our goal to identify effective natural materials for the prevention and treatment of APAP injury, we investigated the liver protective effect of CA-HE50 against APAP-induced liver injury in this study.

Table 2 List of 88 metabolites of CA-HE50 that identified by UHPLC-QTOF/MSMS chromatograms

No	RT (min)	Metabolites	Contents (mg/g)	No	RT (min)	Metabolites	Contents (mg/g)
1	0.98	Stachyose	6.34	**45**	11.11	6-[3-[(3,4-Dimethoxyphenyl)methyl]-4-methoxy-2-(methoxymethyl)butyl]-4-methoxy-1,3-benzodioxole	5.16
2	0.98	D-Gln	5.09	**46**	11.52	13-KODE	5.29
3	0.98	Methyl acrylate derivative	4.62	**47**	11.54	1-Palmitoyl-2-hydroxy-sn-glycero-3-phosphoethanolamine	4.83
4	0.99	Gentianose	6.39	**48**	11.63	Dioctyl sulfosuccinate	5.62
5	0.99	Lansoprazole	4.60	**49**	11.82	1-Palmitoyl-sn-glycero-3-phosphocholine	5.46
6	1.00	Sucrose	5.79	**50**	11.97	9,10-EODE	5.55
7	1.00	D-Fructose	5.40	**51**	12.26	Phosphatidylcholine 14:0–16:0	4.93
8	1.02	Muramate	5.50	**52**	12.32	Glutathione	8.00
9	1.04	Betaine	4.92	**53**	12.42	13-KODE	5.30
10	1.08	Pipecolate	4.44	**54**	12.49	Sorbitan monopalmitate	5.11
11	1.31	L-5-oxoproline	5.63	**55**	12.52	Phosphatidylethanolamine 16:0–20:4	4.92
12	1.33	Adenosine	5.56	**56**	12.54	3,5-Di-tert-butyl-2-hydroxybenzaldehyde	5.04
13	1.33	*β*-leucine	4.80	**57**	12.89	9*Z*,12*Z*,15*Z*-Monolinolenin	4.88
14	1.82	Phenol	5.22	**58**	12.99	Dibutyl phthalate	5.54
15	3.58	Indol-3-lactic acid	4.84	**59**	12.99	Phthalate	4.84
16	5.10	Chlorogenate	5.12	**60**	12.99	Monoisobutyl phthalate	5.14
17	5.11	Caffeate	4.94	**61**	13.37	2-Linoleoylglycerol	4.99
18	6.62	Quercetin-3-glucuronide	5.86	**62**	13.63	9,10-Epoxy-12*Z*-octadecenoic acid	5.78
19	6.62	Spiraeoside	3.93	**63**	13.68	2-Palmitoyl-rac-glycerol	5.91
20	6.63	Quercetin	4.64	**64**	14.09	Linoelaidic acid	5.65
21	6.84	Azelaate	3.49	**65**	14.43	Palmitic acid	4.88
22	6.87	Quercetin 3-*O*-malonylglucoside	2.92	**66**	14.55	1-Stearoyl-rac-glycerol	6.09
23	6.99	Luteolin 7-glucoside	3.62	**67**	14.55	Isostearic acid	4.63
24	7.01	Scutellarin	6.92	**68**	14.60	beta-sitosterol	4.94
25	7.01	Kaempferol	5.10	**69**	14.76	9*Z*,12*Z*,15*Z*-Dilinolenin	5.18
26	7.03	4,5-Dicaffeoylquinic Acid	5.92	**70**	14.95	Phosphatidylcholine 16:1–18:3	4.64
27	7.03	Caffeate	6.83	**71**	15.36	Phosphatidylinositol 18:0–22:4	4.73
28	7.26	Astemizole	3.17	**72**	15.44	9*Z*,11*E*,13*E*-Octadecatrienoic acid ethyl ester	5.09
29	7.30	Madecassoside	6.16	**73**	15.54	Erucamide	6.28
30	7.30	Neohesperidose	5.36	**74**	15.65	Pheophorbide A	5.56
31	7.30	Madecassic acid	6.31	**75**	15.86	Linoleic acid ethyl ester	4.68
32	7.44	Caffeate	5.24	**76**	15.97	Dioctyl phthalate	6.45
33	7.72	Asiaticoside	5.93	**77**	15.97	Pheophorbide A	4.36
34	7.72	3-Oxoursan (28*13) olide	6.40	**78**	16.58	Glycerol tricaprylate	5.00
35	7.72	Rutinose	4.73	**79**	16.60	di-5-nonylphthalate	6.02
36	7.72	NCGC00380457-01!	3.65	**80**	16.92	Cholesterol 3-sulfate	5.56
37	8.46	Quercetin	4.60	**81**	17.04	Fucosterol	4.80
38	8.81	5,6-Dihydroprostaglandin E3	3.17	**82**	17.11	dodecamethylcyclohexasiloxane	4.59
39	9.25	Kaempferol	5.40	**83**	17.23	*β*-Sitosterol	4.89
40	9.61	Madecassic acid	6.42	**84**	17.80	Cyclopropanecarboxamide	5.32
41	10.41	3-Oxoursan (28–13) olide	6.48	**85**	18.83	1-Stearoyl-rac-glycerol	4.11
42	10.41	Asiatic acid	6.62	**86**	19.63	Sphingomyelin d18:0-C16:0	5.48
43	10.76	Propanedinitrile	4.64	**87**	22.65	1,2-Ditetradecanoyl-sn-glycero-3-phospho-1′-sn-glycerol	4.61
44	10.86	Isoalantolactone	4.61	**88**	22.69	Fluticasone propionate	4.89

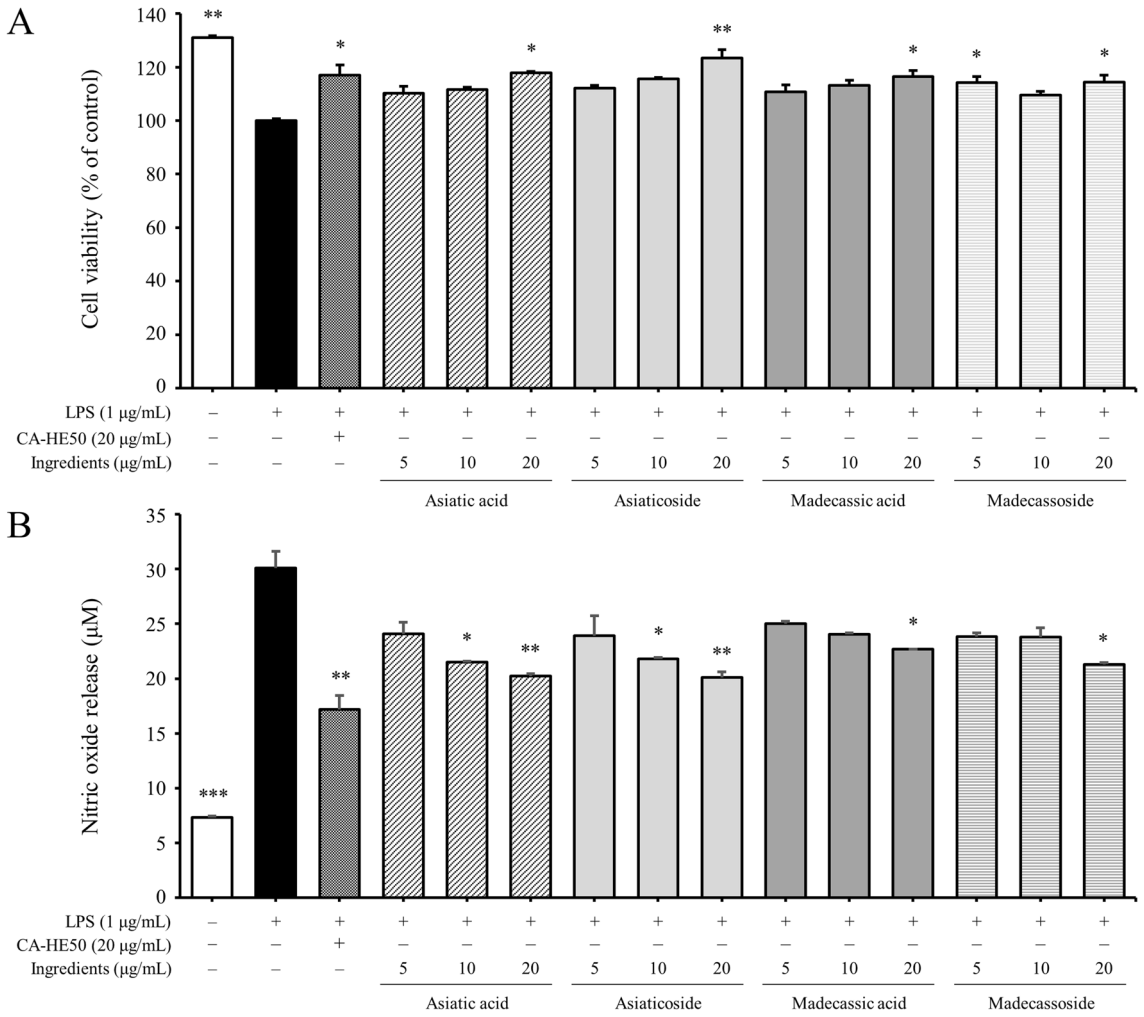

Fig. 6 Measurement of cell viability and NO release. **a** Effects of CA-HE50 and four component ingredients on cell proliferation of RAW 264.7 cells; **b** Effects of CA-HE50, and four constituent components on NO secretion by RAW 264.7 cells. Data are expressed as means ± SEMs ($n = 3$) and were analyzed using one-way ANOVA. *significantly different from LPS control ($p < 0.05$), **significantly different from vehicle control ($p < 0.01$)

We measured levels of the serum liver biomarkers AST, ALT, and LDH as these are the major biochemical markers used to detect early acute liver injury associated with oxidative stress [32]. Administration of APAP significantly increased serum levels of ALT, AST, and LDH compared to the control group and caused severe liver tissue pathological lesions. CA-HE50 pre-treatment dose-dependently decreased the APAP-induced increase in levels of serum ALT, AST, and LDH levels, indicating that CA-HE50 has a protective effect against fulminant liver injury. In addition, histopathological examination confirmed that CA-HE50 significantly attenuated the pathological changes caused by APAP.

Numerous studies have demonstrated that oxidative stress is an important factor that contributes to liver dysfunction in APAP-induced liver injury in mice. APAP-induced oxidative stress can damage proteins, lipids, and DNA, resulting in cellular injury [9]. To assess whether CA-HE50 prevented liver damage through attenuation of oxidative stress, we measured levels of the oxidative stress-related markers GSH and MDA in the liver. GSH, a powerful antioxidant, can protect cells from oxidative injury and reduce injury from APAP overdose [33]. Excess APAP is converted to NAPQI, a toxic substance, by CYP2E1, and NAPQI is then converted into a detoxified form by binding to GSH and released [34], resulting in depletion of GSH. MDA is a biomarker of liver oxidative stress [35]. We found that excessive APAP resulted in oxidative stress in liver tissues as reflected by an increase in MDA content and reduction in GSH level. GSH depletion and MDA overproduction caused by APAP were reversed by CA-HE50 treatment. These results suggest that the liver protective activity of CA-HE50 might be related to

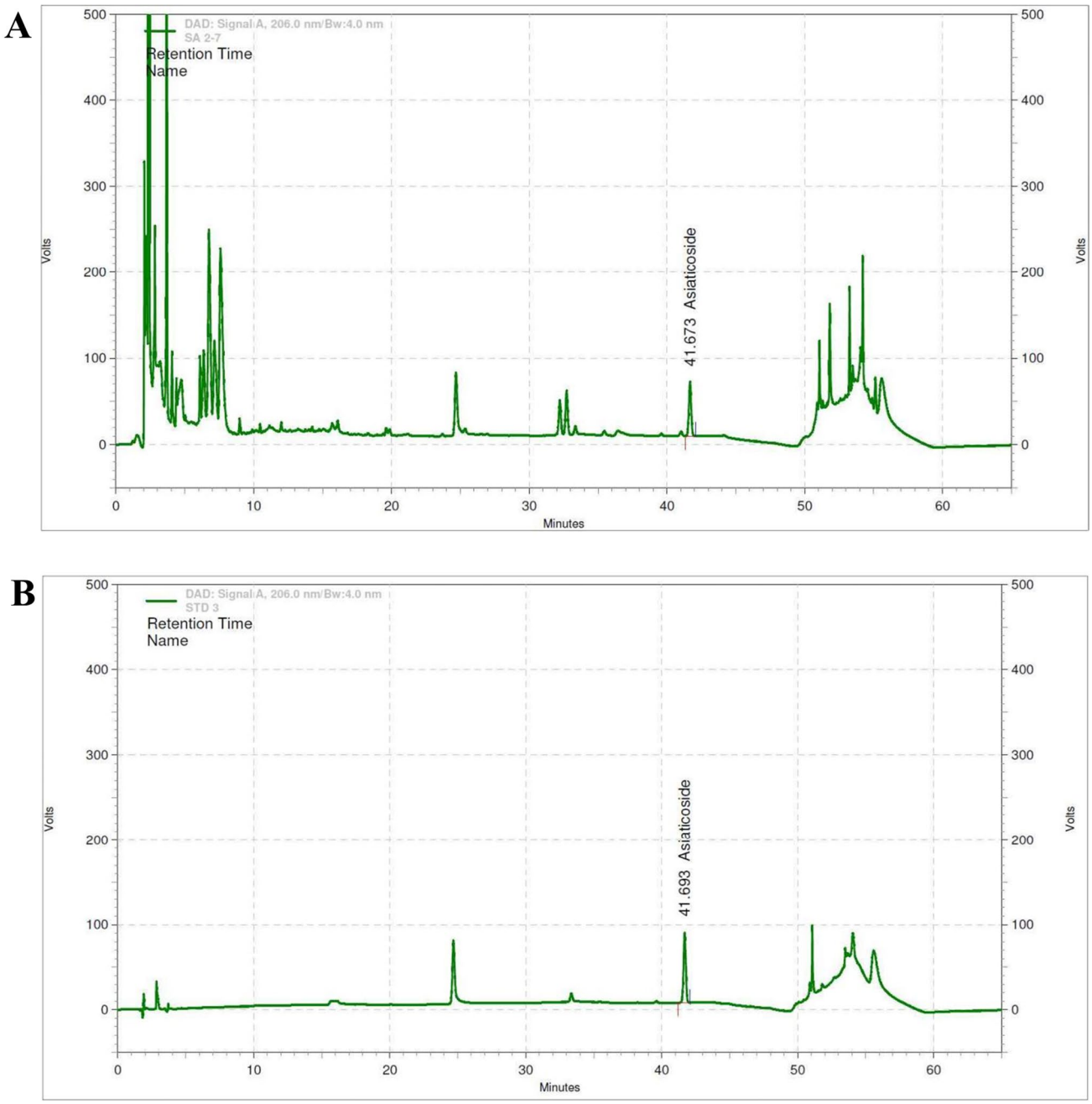

Fig. 7 HPLC chromatogram of *Centella asiatica* 50% ethanol extract (CA-HE50). **a** asiaticoside standard; **b** CA-HE50

its antioxidative capacity. We also confirmed that CA-HE50 effectively decreased transcript expression of CYP2E1.

MCP1 is a cytokine that induces inflammation by recruiting monocytes, memory T cells, and dendritic cells to injured tissue or infection sites [36]. Furthermore, APAP overdose can cause inflammatory cell infiltration and overexpression of pro-inflammatory cytokines (such as TNF-α and IL-1β), ultimately leading to inflammation [37]. We measured mRNA expression levels of MCP1, TNF-α, IL-1β, IL-4, IL-6, and IL-10 in the liver tissue of experimental animals, and confirmed that CA-HE50 inhibited expression of these genes, confirming that the liver protective effect of CA-HE50 was partly attributable to its anti-inflammatory activity.

UHPLC-QTOF/MSMS analysis was conducted to identify phytochemicals present in CA-HE50 that protected against APAP-induced liver toxicity, and four components were identified as functional component candidates. By evaluating the protective and anti-inflammatory efficacy of these components and CA-HE50 using RAW 264.7 cells,

we found that AS was the most effective phytochemical at protecting against APAP-induced cellular injury. Further studies are needed to determine the molecular mechanisms underlying the protective effects of CA-HE50 and AS on liver injury, but our results indicate that CA-HE50 and AS are strong potential candidates to protect against APAP-induced liver injury.

Acknowledgements This work was supported by the Korean Institute of Planning and Evaluation for Technology in Food, Agriculture, Forestry (IPET) through the High Value-Added Food Technology Development Program, funded by the Ministry of Agriculture, Food and Rural Affairs (MAFRA) (117050-3).

Compliance with ethical standards

Conflict of interest The author(s) have no potential conflicts of interest to declare with respect to the research, authorship, and/or publication of this article.

References

1. Jaeschke H, Xie Y, McGill MR (2014) APAP-induced liver injury: from animal models to humans. J Clin Transl Hepatol 2:153–161. https://doi.org/10.14218/JCTH.2014.00014
2. Woolbright BL, Jaeschke H (2017) Role of the inflammasome in APAP-induced liver injury and acute liver failure. J Hepatol 66:836–848. https://doi.org/10.1016/j.jhep.2016.11.017
3. Bunchorntavakul C, Reddy KR (2013) APAP-related hepatotoxicity. Clin Liver Dis 17:587–607. https://doi.org/10.1016/j.cld.2013.07.005
4. Herndon CM, Dankenbring DM (2014) Patient perception and knowledge of APAP in a large family medicine service. J Pain Palliat Care Pharmacother 28:109–116. https://doi.org/10.3109/15360288.2014.908993
5. Clark R, Fisher JE, Sketris IS, Johnston GM (2012) Population prevalence of high dose paracetamol in dispensed paracetamol/opioid prescription combinations: an observational study. BMC Clin Pharmacol 12:11. https://doi.org/10.1186/1472-6904-12-11
6. Lancaster EM, Hiatt JR, Zarrinpar A (2014) APAP hepatotoxicity: an updated review. Arch Toxicol 89:193–199. https://doi.org/10.1007/s00204-014-1432-2
7. Kane AE, Mitchell SJ, Mach J (2016) APAP hepatotoxicity in mice: effect of age, frailty and exposure type. Exp Gerontol 73:95–106. https://doi.org/10.1016/j.exger.2015.11.013
8. Murray KF, Hadzic N, Wirth S, Bassett M, Kelly D (2008) Drug-related hepatotoxicity and acute liver failure. J Pediatr Gastroenterol Nutr 47:395–405. https://doi.org/10.1097/MPG.0b013e3181709464
9. Jaeschke H, McGill MR, Ramachandran A (2012) Oxidant stress, mitochondria, and cell death mechanisms in drug-induced liver injury: lessons learned from APAP hepatotoxicity. Drug Metab Rev 44:88–106. https://doi.org/10.3109/03602532.2011.602688
10. Nourjah P, Ahmad SR, Karwoski C, Willy M (2006) Estimates of APAP (Paracetomal)-associated overdoses in the United States. Pharmacoepidemiol Drug Saf 15:398–405. https://doi.org/10.1002/pds.1191
11. Miller LL, Bly CG, Watson ML, Bale WF (1951) The dominant role of the liver in plasma protein synthesis, a direct study of the isolated perfused rat liver with the aid of lysine-ϵ-C14. J Exp Med 94:431–453. https://doi.org/10.1084/jem.94.5.431
12. Shaabana HAE, El-Ghoraba AH, Shibamotob T (2012) Bioactivity of essential oils and their volatile aroma components: review. J Essent Oil Res 24:203–212. https://doi.org/10.1080/10412905.2012.659528
13. Jamil SS, Nizami Q, Salam M (2007) *Centella asiatica* (Linn.) urban o' a review. Nat Pro Radiance 6:158–170. https://doi.org/10.1084/jem.94.5.431
14. Zahara K, Bibi Y, Tabassum S (2014) Clinical and therapeutic benefits of Centella asiatica. Pure Appl Biol 3:152–159. https://doi.org/10.19045/bspab.2014.34004
15. Fontana RJ (2008) Acute Liver Failure including Aceteaminophen overdose. Med Clin North Am 92:761–794. https://doi.org/10.1016/j.mcna.2008.03.005
16. Roberts DW, Bucci TJ, Benson RW, Warbritton AR, McRae TA, Pumford NR, Hinson JA (1991) Immunohistochemical localization and quantification of the 3-(cystein-S-yl)-acetaminophen protein adduct in acetaminophen hepatotoxicity. Am J Pathol 138:359–371.
17. McGill MR, Sharpe MR, Williams CD, Taha M, Curry SC, Jaeschke H (2012) The mechanism underlying APAP-induced hepatotoxicity in humans and mice involves mitochondrial damage and nuclear DNA fragmentation. J Clin Invest 122:1574–1583. https://doi.org/10.1172/JCI59755
18. Xie Y, McGill MR, Dorko K, Kumer SC, Schmitt TM, Forster J, Jaeschke H (2014) Mechanisms of APAP-induced cell death in primary human hepatocytes. Toxicol Appl Pharmacol 279:266–274. https://doi.org/10.1016/j.taap.2014.05.010
19. Kato GJ, McGowan V, Machado RF, Little JA, Taylor J, Morris CR, Nichols JS, Wang X, Poljakovic M, Morris SM Jr, Gladwin MT (2006) Lactate dehydrogenase as a biomarker of hemolysis-associated nitric oxide resistance, priapism, leg ulceration, pulmonary hypertension, and death in patients with sickle cell disease. Blood 107:2279–2285. https://doi.org/10.1182/blood-2005-06-2373
20. Tomasi TB Jr, Tisdale WA (1964) Serum gamma-globulins in acute and chronic liver diseases. Nature 201:834–835. https://doi.org/10.1038/201834a0
21. Li S, Tan HY, Wang N, Zhang ZJ, Lao L, Wong CW, Feng Y (2015) The role of oxidative stress and antioxidants in liver diseases. Int J Mol Sci 16:26087–260124. https://doi.org/10.3390/ijms161125942
22. Liu WX, Jia FL, He YY, Zhang BX (2012) Protective effects of 5-methoxypsoralen against APAP induced hepatotoxicity in mice. World J Gastroenterol 18:2197–2202. https://doi.org/10.3748/wjg.v18.i18.2197
23. Milton PS, Muthumani M, Shagirtha K (2013) Quercetin potentially attenuates cadmium induced oxidative stress mediated cardiotoxicity and dyslipidemia in rats. Eur Rev Med Pharmacol Sci 17:582–595. https://doi.org/10.1007/s12012-013-9227-x
24. Wan J, Gong X, Jiang R, Zhang Z, Zhang L (2013) Antipyretic and anti-inflammatory effects of asiaticoside in lipopolysaccharide-treated rat through up-regulation of heme oxygenase-1. Phytother Res 27:1136–1142. https://doi.org/10.1002/ptr.4838
25. Shukla A, Rasik AM, Dhawan BN (1999) Asiaticoside-induced elevation of antioxidant levels in healing wounds. Phytother Res 13:50–54. https://doi.org/10.1002/(SICI)1099-1573(199902)13:1<50::AID-PTR368>3.0.CO;2-V
26. Shao W, Cao X, Shen L, Zhang F, Yu B (2017) A convergent synthesis of the triterpene saponin asiaticoside. Asian J Org Chem 6:1270–1276. https://doi.org/10.1002/ajoc.201700153
27. Huang YH, Zhang SH, Zhen RX, Xu XD, Zhen YS (2004) Asiaticoside inducing apoptosis of tumor cells and enhancing antitumor activity of vincristine. Ai Zheng 23:1599–1604.
28. Park DW, Jeon H, So R, Kang SC (2020) Centella asiatica extract prevents visual impairment by promoting the production

of rhodopsin in the retina. Nutr Res Pract 14:203–217. https://doi.org/10.4162/nrp.2020.14.3.203
29. Nourjah P, Ahmad SR, Pharm CK, Willy M (2006) Estimates of acetaminophen (paracetomal)-associated overdoses in the United States. Pharmacoepidemiol Drug Saf 15:398–405. https://doi.org/10.1002/pds.1191
30. Rubin JB, Hameed B, Gottfried M, Lee WM, Sarkar M (2018) Acute liver failure study group. Acetaminophen-induced acute liver failure is more common and more severe in women. Clin Gastroenterol Hepatol 16:936–946. https://doi.org/10.1016/j.cgh.2017.11.042
31. McNulty R, Lim JME, Chandru P, Gunja N (2018) Fewer adverse effects with a modified two-bag acetylcysteine protocol in paracetamol overdose. Clin Toxicol (Phila) 56:618–621. https://doi.org/10.1080/15563650.2017.1408812
32. Uchida NS, Silva-Filho SE, Aguiar RP, Wiirzler LAM, Cardia GFE, Cavalcante HAO, Silva-Comar FMS, Becker TCA, Silva EL, Bersani-Amado CA, Cuman RKN (2017) Protective effect of cymbopogon citratus essential oil in experimental model of acetaminophen-induced liver injury. Am J Chin Med 45:515–532. https://doi.org/10.1142/S0192415X17500318
33. Yan M, Huo Y, Yin S, Hu H (2018) Mechanisms of acetaminophen-induced liver injury and its implications for therapeutic interventions. Redox Biol 17:274–283. https://doi.org/10.1016/j.redox.2018.04.019
34. Du K, Ramachandran A, Jaeschke H (2016) Oxidative stress during acetaminophen hepatotoxicity: sources, pathophysiological role and therapeutic potential. Redox Biol 10:148–156. https://doi.org/10.1016/j.redox.2016.10.001
35. Liang H, Feng Y, Cui R, Qiu M, Zhang J, Liu C (2018) Simvastatin protects against acetaminophen-induced liver injury in mice. Biomed Pharmacother 98:916–924. https://doi.org/10.1016/j.biopha.2017.12.076
36. Deshmane SL, Kremlev S, Amini S, Sawaya BE (2009) Monocyte chemoattractant protein-1 (MCP-1): an overview. J Interferon Cytokine Res 29:313–326. https://doi.org/10.1089/jir.2008.0027
37. Wang L, Li X, Chen C (2018) Inhibition of acetaminophen-induced hepatotoxicity in mice by exogenous thymosinβ4 treatment. Int Immunopharmacol 61:20–28. https://doi.org/10.1016/j.intimp.2018.05.011